1980

A deuterium nuclear magnetic resonance study of chain disorder in lamellar potassium palmitate: The effect of long and short chain guests

Peter A. Beckmann
Bryn Mawr College, pbeckman@brynmawr.edu

E. E. Burnell

M. A. Heldman

K. R. Northey

T. P. Higgs

A deuterium nuclear magnetic resonance study of chain disorder in lamellar potassium palmitate: The effect of long and short chain guests

P. A. Beckmann, E. E. Burnell, M. A. Heldman, K. R. Northey, and T. P. Higgs

Abstract: The deuterium magnetic resonance spectra of lamellar phases of host perdeuterated potassium palmitate mixed with varying amounts of guest protiated potassium octanoate and behenate and 86.3 mol% D_2O are reported. At higher temperatures, the short chain guests give rise to more fluidity and the long chain guests give rise to less fluidity towards the end of the host chain. At low temperatures there are changes in the interaction between the polar head group and the water which depend on sample composition. The transition from the lamellar phase to the low temperature gel phase is investigated and in some cases the gel phase is found to be a complicated many-phase region, at least for the water. The spectral results are presented in detail but compact and empirical methods of analysis are also investigated.

I. Introduction

Mixtures of fatty acid salts and water form a variety of lyotropic crystalline phases (1) which are of great interest in surface and interface science. The liquid crystalline or L_α lamellar phase is of particular interest because the bilayer arrangement of the soap molecules is the same as that formed by the phospholipids of biological membranes. Such a model is greatly oversimplified since real biological membranes also contain proteins imbedded in the bilayer, and in addition the phospholipids have various chain lengths. This paper addresses the latter complication. We have studied the effect that added guest soap molecules of differing chain lengths have on the molecular order of a more abundant host soap molecule. In particular, we have investigated the fluidity of the lipid chains in perdeuterated potassium palmitate $(CD_3(CD_2)_{14}$, COOK in the presence of varying amounts of protiated potassium octanoate $CH_3(CH_2)_{20}COOK$. It has been found that for low mole fraction of guest molecules the mean area per polar head in the L_α phase is not affected whereas when the mole fraction of guests exceeds about 20% the lamellar phase is no longer stable (2). In our experiments, concentrations of the guest molecule are sufficiently low that the lamellar nature of the system is not affected.

The experimental techniques is Fourier transform quadrupolar echo deuteron magnetic resonance spectroscopy (3). The non-zero electric field gradients at the deuterium nuclei lead to quadrupolar splittings of the nmr lines. These splittings are large compared with the broadening resulting from dipolar interactions and magnetic field inhomogeneities and depend on the degree to which the quadrupolar interactions are averaged out by the molecular motion. Thus one obtains a deuterium nmr spectrum with small splittings for the CD_3 deuterons at the end of the chain where there may be consideration motion and large splittings for the α deuterons where there is considerably less motion (4).

Studies related to those presented here have appeared in the literature. Lamellar phases of mixtures of potassium decanoate, meristate, and stearate at 60°C have been studied (5) and it was found that there is little change in the methylene chain deuterium splittings upon addition of guest molecules. The deuterium splitting of the *a* position in fatty acids and fatty acid salts dissolved in small concentrations in orienting lyotropic liquid crystals has been measured (6),

and for short chain lengths a linear dependence of splitting on chain length was observed. These studies did not examine the temperature dependence of the splittings, as is done in the present study.

II. Experimental

Palmitic acid (Sigma Chemical Co., Sigma grade, 99%) was used to prepare palmitic-d_{31} acid as discussed elsewhere (7). The deuterated acid was purified by silica gel chromatography. The incorporation of deuterium was found to be greater than 98.5% by high resolution nmr and mass spectrometric analysis.

The potassium salts were precipitated from ethanol by the addition to the corresponding fatty acids of 1 equiv. of potassium hydroxide in concentrated aqueous solution. The potassium salts were then recrystallized from ethanol and vacuum dried at room temperature to yield the soap as a fluffy white solid.

Several samples of 6.3 mol D_2O to 1 mol soap were prepared by weighing the soap and D_2O to 1% accuracy into a constricted Pyrex sample tube. The soap was mainly potassium palmitate, but also contained 0, 0.01, 0.05, or 0.20 mol of potassium octanoate or potassium behenate per mole total soap. For reference, Table 1 lists the composition of the various mixtures used, along with a code which will be used hereafter to identify the various samples. Samples were mixed by centrifuging many times through the constriction in the sealed glass tube used for nmr. It should be noted that even after 50 such mixings spectral changes were observed to occur on further mixing; hence, samples were mixed (typically >100 times) until no further spectral changes occurred.

Deuterium nmr spectra were obtained as a function of temperature in the lamellar and lower temperature phases at 13.8 MHz with a Bruker SXP 4-100 pulsed nmr spectrometer by Fourier transforming the signal starting at the top of the quadrupolar echo (3). Spectra were run on resonance and Fourier transformation gave half of the symmetric spectrum. The spectra obtained for 0% guest differ slightly from those previously reported (8-10). These differences were traced via mass spectrometry to a greater amount of different chain length fatty acids (e.g., stearic acid) in the palmitic acid (supplied from Sigma Chemical Co.) which was used to prepare the perdeuterated potassium palmitate. For the present study we are interested only in changes which occur upon addition of different chain length fatty acid salts, and hence the minor differences compared with previous work need not concern us further. The present set of samples forms a useful basis for the comparisons of interest.

III. Results and Discussions

The deuterium nmr of the six samples indicated in Table 1 has been studied as a function of temperature in the L_α and some lower temperature gel or L_β phases. First, we discuss the results for the lower temperature phases. These results were obtained mainly to determine the phase transition temperature which is useful for comparing the results from the different samples as a function of reduced temperature in the L_α phase.

A. Low Temperature Phases and Phase Transition

When comparing samples of different composition, it is useful to measure temperature with respect to the critical temperature T_c which we define as the temperature on the cooling

curve at which the first sign of a non-L_α phase spectrum appears. Thus we define the reduced temperature T_r by $T_r = T - T_c$. We have found it convenient to use two methods of estimating T_c. The first method utilizes the signal from the CD_2's in the gel phase and the second method is based on the changes in signal from the D_2O.

  The first method is illustrated by Fig. 1 which shows the spectrum from a mixture of the L_α and gel phases for the 5% C_{2Z} sample at 36.5°C. Although we call all lower temperature phases gel phases, their actual structure is uncertain. The large intensity peak below 2 kHz (off-scale) in Fig. 1 is from the D_2O. This peak obscures the CD_3 signal in both Figs. 1 and 2. The resolved peaks between 5 and 16 kHz are from the L_a region and correspond to the 90° powder pattern edges due to the different CD_2's in the hydrocarbon chain (8). These peaks from the CD_2's in the L_α phase manifest themselves much more clearly at higher temperatures as shown in Fig. 2 which corresponds to the same sample (5%, C_{22}) at 145°C. The broad signal with a cut-off in the vicinity of 30 kHz in Fig. 1 is typical of methylene chains in a gel or L_β phase region (8). (This signal does contain a small contribution from the wings of the L_α phase spectrum but this contribution will not affect our analysis seriously.) To obtain information about the percent of gel in the two phase region and also to define the phase transition temperature T_c, we integrate a region of the broad gel spectrum. The lower limit of integration is chosen so as to minimize the contribution of the L_α phase spectrum wings. Integrals plotted vs. T serve to define both T_c and the composition of the two phase regions.

  The second method of studying the phase transition involves observing the D_2O signal as a function of temperature. T_c is readily obtained from the first appearance of the gel D_2O signal on cooling. This method is illustrated in Fig. 3 for the 20% C_{22} sample. Not only is this a very sensitive way of defining T_c, but it also demonstrates that in several cases the gel is a multiphase region, at least as far as the water is concerned. The 0.5 and 1.8 kHz peaks in the two highest temperature spectra in Fig. 3 are the signals from D_2O and the palmitate CD_3 respectively in the L_α phase. The peaks at 0, 1.1., and 1.6 kHz in the lowest temperature spectrum in Fig. 3 are assumed to be signals from three types of D_2O in the gel phase. On cooling, the first detected gel phase D_2O peak in the spectra of both 20% C_{22} and 20% C_8 samples appears to have zero splitting, which indicates that there is D_2O in an isotropic environment such as patches of bulk water. Whereas there appear to be at least three D_2O gel phase environments for the 20% C_{22} sample (Fig. 3), and at least two for the 20% C_8 sample, there is only one gel phase D_2O environment for the 0% sample. For the latter sample, an isotropic D_2O peak was not observed. (We note that for another 0% sample, an isotropic phase D_2O peak was observed at 30°C (9).) As demonstrated in Fig. 3, the growth and decay of the various D_2O phases on cooling is easily followed by deuterium nmr. For. potassium palmitate in the presence of guest chains, this illustrates that for the water at least, the "gel" phase is a complicated many-phase region. Another interesting feature of the "mixed phase" region will be discussed in the following section after presentation of Figs. 5 and 6.

  T_c for each sample has been estimated by the two methods outlined here and the values are given in Table 1. We note that recently another powerful way of measuring phase transition temperatures using the method of moments has been reported (11).

B. L_α Phase

  The deuterium nmr of the D_2O and the potassium palmitate host in the six samples has been used to obtain the spectral splittings, $\Delta\nu$, between the two 90° powder pattern singularities of the D_2O, the CD_3 and each CD_2 deuterium as a function of temperature in the L_α phase. A

sample spectrum, with the spectral peaks identified by their position along the chain, is shown in Fig. 2, We have assumed that all our spectra are indeed from samples in a true lamellar phase. The opposite direction and moderate size of the changes observed with different chain length guests support this assumption. There are certainly no changes to a cubic or hexagonal phase (1): these would be associated with a drastic reduction in spectral splittings (12). We shall examine several ways of comparing results from the different samples and of handling the more than 1000 measured splittings. Starting from the spectral splitting as a function of carbon position, we discuss results for the different samples for two values of T_r, one near the phase transition and the other at a higher temperature. As is the case throughout this study, results from the 1% C_{22} and 1% C_8 samples did not differ, within experimental error, from those for the 0% sample and for clarity we omit those points from most graphs. Also, a general result is that the splittings for the *5%* C_{22} sample were always between those for the 0% and 20% C_{22} samples, as might be expected for a dilution effect.

However, the differences were not always linear and we include the data from the 5% C_{22} sample in most plots.

Figure 4IaI shows the spectral splittings Δv at two reduced temperatures as a function of carbon positions in the host perdeuterated potassium palmitate for the 0%, 5% C_{22}, 20% C_{22}, and 20% C_8 samples. In order to see some of the effects on the host of the long and short chain guests more easily, Fig. 4*b* shows the ratios of the splittings in the 5% and two 20% samples to the splittings in the 0% sample. The lines joining data points in Fig. 4 are for visual clarity only. At low temperatures, the addition of either long or short chain farry acid salt guests increases spectral splittings in the host (for all except the α position of 20% C_8 where there is a slight decrease). At higher temperatures, the addition of long chain guests gives rise to an increase in spectral splitting (beyond the carbon 4 position) whereas the addition of short chain guests gives rise to a decrease in spectral splittings. The high temperature result for carbons 5 to 15 might be expected intuitively on the basis of chain packing, as one might expect the 16-carbon chain to have more freedom to move in the presence of short chains and less freedom in the presence of long chains. The low temperature results and the high temperature polar region results are probably associated with differing interactions between lipid and water for the different samples. This is discussed more fully in the following paragraph.

Plots such as those in Fig. 4 allow a comparison of chain order from one position to the next at specific temperatures. Another informative way of presenting the data is to choose various CD_2 positions and to examine the splittings as a function of reduced temperature. This is done in Fig. 5 for the carbon 2, carbons 5 and 6, carbon 10, and carbon 15 positions. The D_2O splittings are much smaller than the CD_2 splittingsand are shown in Fig. 6. In Figs. 5 and 6, part *a* shows the splittings of the 0%, 5% C_{22}, 20% C_{22}, and 20% C_8 samples and part *b* shows the ratio of the splittings of the latter three to those of the 0% sample. At high temperatures and toward the methyl end of the chain the results are as expected from the previous arguments about chain packing. The results for the 2 position (Fig. 5) and for the D_2O (Fig. 6) are quite striking, however, in that the 0% sample always has the greatest splitting at high temperature. As has been discussed elsewhere (9), the reduction of spectral splittings are not necessarily associated with greater mobility of the system, but may merely reflect changes in the preferred angle that a part of the molecule makes with the normal to the plane of the bilayer. Our results, then, imply: (*a*) that the palmitate has greater mobility at the head group in the presence of guest chains, as might be expected if the planar arrangement of the carbonyl groups is distorted because of the heterogeneity of chain lengths; and (or) (*b*) that the addition of guests alters the distribution of

orientations that the first C—C bonds and the D_2O make with the normal to the bilayer. Additionally, for both the 0% and 5% C_{22} samples, the splittings of the carbon 2 position and the D_2O first rise with increasing temperature and then fall; this observation has been attributed to changes in the interaction between lipid and water (9). However, for the 20% samples the 2 position splittings decrease with increasing temperature, but the water shows an increase and then a decrease. In the spirit of the model of of ref. 9, these results indicate a different interaction between the lipid and the water in the 20% samples than in the 0% sample. Qualitatively, the following picture can explain these results. The presence of mixed chain lengths with altered packing requirements inside the bilayer may well disturb the planar arrangement of the carboxyl groups. The orientation of water molecules which are hydrogen bonded to two carboxyl groups will then change, leading to an orientation that gives a lower splitting. The orientation of the water molecules may well change with temperature leading to the observed rise and fall of the D_2O splittings relative to the lamellar normal. However, this change in orientation of the D_2O is not necessarily associated with similar changes in the orientation of the head groups. Such a situation would explain the observed splittings. It should be pointed out that the above model is somewhat crude, and that at the moment we have not studied the deuterium spectral splittings of the guest chains.

The water splittings are an average over many water environments and it is difficult to make more than qualitative comparisons between lipid and water spectral parameters.

It is convenient, at this stage, to point out an interesting feature of the "mixed phase" region $(T_r < 0)$ for the 20% C_{22} sample (solid triangles in Figs. 5a and 6a). Except for the 2 position, the 20% C_{22} splittings for the L_α component have a maximum at $T = T_c$ $(T_r = 0)$ in Fig. 5a. That the splittings decrease on decreasing temperature below T_c is presumably due to the L_a component of the mixed phase region becoming richer in the host palmitate as the sample is cooled. The splittings are approaching the lower values observed for the 0% sample. The behavior of the D_2O signal (Fig. 6a) from the L_α phase region below T_c is also in agreement with this interpretation.

Examination of Figs. 4-6 is fruitful but these figures present only part of the results and focus on only one aspect of the lipid ordering at a time. We shall next examine convenient ways to compare all CD_2 splittings on a single plot. To do so, we define the average splitting $\langle \Delta v \rangle$, the mean square splitting $\langle (\Delta v)^2 \rangle$ and the distribution parameter Δ_2 by

[1] $\quad \langle \Delta v \rangle = \frac{1}{14} \sum_{i=2}^{15} \Delta v_i$

[2] $\quad \langle (\Delta v)^2 \rangle = \frac{1}{14} \sum_{i=2}^{15} (\Delta v_i)^2$

[3] $\quad \Delta_2 = \frac{\langle (\Delta v)^2 \rangle}{\langle \Delta v \rangle^2} - 1$

The average splitting $\langle \Delta v \rangle$ and the distribution parameter Δ_2 are plotted as function of reduced temperature in Figs, 7 and 8 respectively. The plots in Fig. 7 for $\langle \Delta v \rangle$ are very similar to those for positions 10 and 15 in Fig. 5a and the previous arguments about lipid packing and the lipid-water interaction can again be used to interpret the results. The plot in Fig. 8 for Δ_2 is a compact and particularly useful way to present the results. (The distribution parameter Δ_2 has Deen discussed in detail elsewhere (11).) For example, a value of $\Delta_2 = 0$ means that all splittings are equal and the greater the value of Δ_2 the greater is the distribution in the splittings along the chain. In fact much information on the average order parameter profile is contained in Fig. 8. It is immediately obvious that the spectral peaks spread out at higher temperatures; or, as observed

previously (8), the "plateau" in the splittings versus position curve disappears. Also, the 20% C_8 and 0% samples are seen to have a similar distribution of splittings at all temperatures, while the 20% C_{22} sample has less spread in peak positions at all values of T_r. These observations can also be made by close inspection of the many curves given for a limited temperature range in Fig. 4*a* but the comparisons are more convenient with the condensation of the entire set of results represented by Figs. 7 and 8. However, Figs. 4-6 are most useful in examining specific areas of interest; for example the averaging involved in Figs. 7 and 8 tend to hide some of the interesting features of the polar head region.

Another way of examining the results is to look at ratios of various splittings. Such ratios do not give any information about the magnitude of the orientational order of the chain, but they show instead the relative order of different parts of the chain, and how that relative order changes upon addition of guest chains. To demonstrate this, we plot in Fig. 9 the ratios of splittings for positions 10 to 15 versus T_r for the various samples. The ratio of couplings, $\Delta v_{10}/\Delta v_{15}$, clearly demonstrates that, relative to the middle of the chain, the methyl end is less ordered in the presence of short chains and more ordered in the presence of long chains at all temperatures. This result is reasonable since long chain guests would restrict the motions of the host methyl end while with the short chain guest, the host methyl end has more room to move about than it does in the 0% sample.

Ratios of nmr splittings of one part of a chain to those of another part have recently been used in an interesting way (13). The basis of the treatment is to describe the order parameter for a CD bond as the product of molecular and conformational order parameters (13,14). In practice, this separation cannot be performed quantitatively because there is no way to measure one of the order parameters separately. Also, the concept of a unique molecular order parameter matrix in soap and liquid crystal systems may not be valid (15) (and private communication by E. Samulski) because it implies that one can do time averages over the molecular and conformational motions independently (15). However, it is useful to employ this conformational motions independently (15). However, it is useful to employ this method of analysis since it provides an empirical way of treating the results, at least for some chain positions. For a uniaxial phase, the model employs two order parameters, and it suggests that the splitting Δv_i for the *i*th CD_2 can be related to the splittings of any other two CD_2 splittings Δv_j, and Δv_k by the equation (13)

[4] $\quad \Delta v_i = C_{jk}{}^i \Delta v_j + C_{kj}{}^i \Delta v_k$

where the $C_{jk}{}^i$ are functions of the conformational order parameters in this model. If the $C_{jk}{}^i$ are independent of temperature, plots of $\Delta v_j /\Delta v_k$ versus $\Delta v_j /\Delta v$ will give straight lines with slope $C_{jk}{}^i$ and intercept $C_{jk}{}^i$ as observed in ref. 13. In such a situation one can use [4] as an empirical equation in spite of the objections raised above. We have applied this method to the case for $j = 10$ and $k = 15$ and plotted the equation

[5] $\quad \dfrac{\Delta v_i}{\Delta v_{15}} = C_{10,15}{}^i \dfrac{\Delta v_{10}}{\Delta v_{15}} + C_{15,10}{}^i$

for *all* chain positions for *each* sample. The experimental points can be approximated with straight lines and least-squares fits to [5] give values of $C_{10,15}{}^i$ and $C_{15,10}{}^i$. The largest deviation from linearity is obtained for the 20% C_8 sample, where there are slight breaks and changes in curvature in the plots. These effects could be due to phase transitions reported in ref. 10. Although this limits the universality of the approach, these changes are not sufficient to affect the general use of the empirical procedure. The case of $i = D_2O$ was also considered since D_2O is

expected to be hydrogen- bonded to the polar head group. This case does not give linear fits, indicating that the $C_{10,15}{}^{D_2O}$ and $C_{15,10}{}^{D_2O}$ do depend on temperature. This is not surprising since specific interactions between D_2O and the polar head group are strongly temperature dependent, as discussed previously.

       This method of analysis is useful for several reasons. It can serve to identify inconsistent assignments of peaks which would show up as deviations from linearity. This is especially helpful in regions of the deuterium nmr spectra where many splittings are almost equal. Also, the $C_{jk}{}^{i}$ values can be used to condense spectral information. The 13 pairs of numbers $C_{10,15}{}^{i}$ and $C_{15,10}{}^{i}$, in conjunction with the $i = 10$ and $i = 15$ parts of Fig. 5a, can serve to reconstruct, at least qualitatively, all the spectral results for the soap chains.

       The most interesting result of this analysis is that the values of $C_{10,15}{}^{i}$ and $C_{15,10}{}^{i}$ change by up to 50% from sample to sample in a consistent way. This change with sample is demonstrated in Fig. 10 for $i = 2, 7,$ and 12. We note that the 1% C_8 and 1% C_{22} samples are represented in this plot whereas they have not appeared previously. Four of the six plots in Fig. 10 are roughly linear, and, what is even more interesting the slopes are of equal and opposite sign for short and long chains as indicated by the dashed lines. Hence, this analysis is useful in comparing the order of the palmitate chain in the presence of other soap chains in a manner that is temperature independent. In terms of the model used (13), the changes in $C_{ik}{}^{j}$ would indicate systematic differences in the conformational order parameters of the palmitate chains in the various mixtures. From the empirical viewpoint, the changes serve to characterize the sensitivity of the potassium palmitate L_α phase to disturbances by added short and long chain molecules.

IV. Conclusion

       We have presented deuterium nmr results for perdeuterated potassium palmitate D_2O mixtures in the presence of varying amounts of potassium octanoate and potassium behenate. The presence of the guest molecule alters the order of the hydrocarbon chain of the host molecule. At higher temperature, the short chain guest leads to a reduced order for the host, while the long chain guest has the opposite effect for all except the head of the host. At low temperature the interaction between lipid and water would seem to be very important in determining the overall host chain spectral parameters. This interaction appears to change the average angle that the first C—C bond makes with the normal to the plane of the bilayer, and hence affects the splittings for all chain positions. The presence of soaps of differing chain lengths would seem to cause changes in the lipid-water interactions, possibly because the presence of these chains distorts the arrangement of the polar heads with respect to the bilayer plane. The details of the interactions involved in the polar head region should be further studied using an alternative approach such as with proton spin labelling techniques (16).

       At lower temperatures there exists a multiphase gel region for the samples containing mixtures of fatty acids. Although the hydrocarbon chain deuteriums give the same spectrum in this temperature range for all samples, the D_2O signal is a useful probe for this region, as separate resonances are observed for the D_2O in different gel regions. From the CD_2 signal, quantitative information about the mixed phase region is obtainable.

       The most instructive extension of this work would be to study the guest molecules in the way the host molecules have been investigated here.

References

1. P. EKWALL, *Adv. Liq. Cryst.* 1, 1 (1975).
2. J. CHARVOLJN and B. MELY. *Mol. Cryst. Liq. Cryst. Lett.* 41,209(1978).
3. J. H. DAVIS, K. R. JEFFREY, M. BLOOM, M. L VALIC, and T. P. HIGGS, *Chem. Phys. Lett.* 42,390(1976).
4. J. CHARVOLIN, P. MANNEVILLE, and B. DELOCHE. *Chem. Phys. Lett.* 23, 345 (1973).
5. B. ME'LY and J. CHARVOLIN. Colloque C.N.R.S., June 1978. In press.
6. D. M. CHEN, F. Y. FUJIWARA, and L. W. REEVES. *Can. J. Chem.* 55,2404 (1977).
7. C. Y. Y. HSIAO, C. A. OTTAWAY, and D. B. WETLAUFFER. *Lipids*, 9, 913 (1974).
8. J. H. DAVIS and K. R. JEFFREY. *Chem. Phys. Lipids*, 20,87 (1977).
9. K. BDOLALL, E, E, BURNELL, and M, Í. VALIC. *Chem. Phys. Lipids*, 20, 115(1977),
10. N. A. P. VAZ, J. W. DOANE, and M. E. NEUBERT. *Phys. Rev. Lett.* 42, 1406(1979).
11. M. BLOOM, J. H. DAVIS, and F. W. DAHLQUIST. To be published; I. H. DAVIS. *Biophys. J*. 27,339(1979).
12. B. MÉLY and J. CHARVOLIN. *Chem. Phys. Lipids*, 19, 43 (1977).
13. P. J. Bos and J. W. DOANE. *Phys. Rev. Lett*. 40,1030(1978).
14. B. DELOCHE and J. CHARVOLIN. *J. Phys. Lett.* 41, L39 (1980).
15. E. E. BURNELL and C. A. DE LANQE. *J. Magn. Reson*. 39, 461 (1980).
16. T. P. HIGGS and A. L. MACKAY. *Chem. Phys. Lipids*, 20, 105(1977).
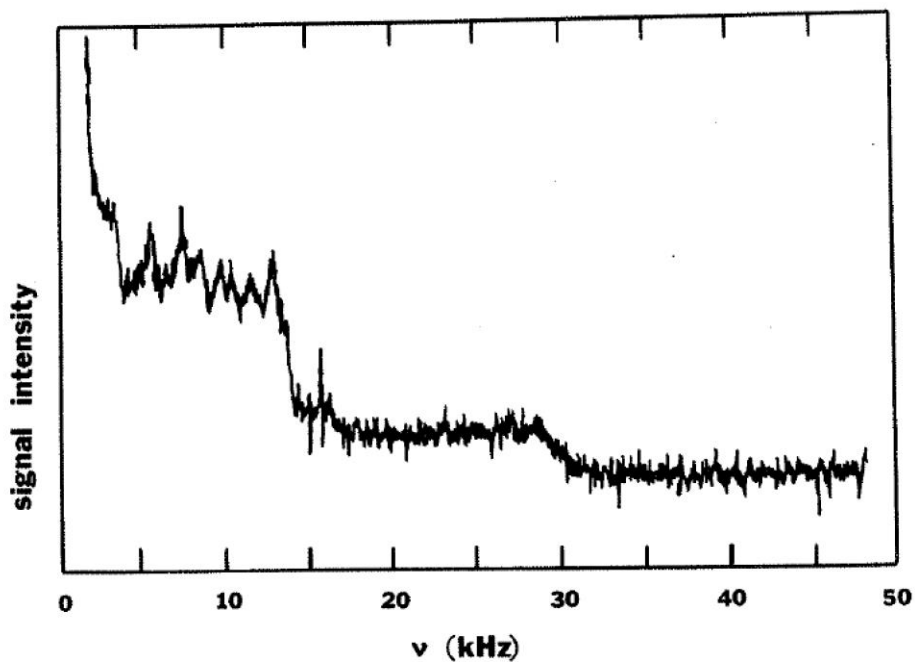
Figures

FIG. 1. The deuterium nmr spectrum of the mixture of lamellar and gel phases of the 5% C_{22} sample (see Table 1) at 36.5°C. Only one half of the symmetric spectrum is shown with spectrum center at 0 kHz.
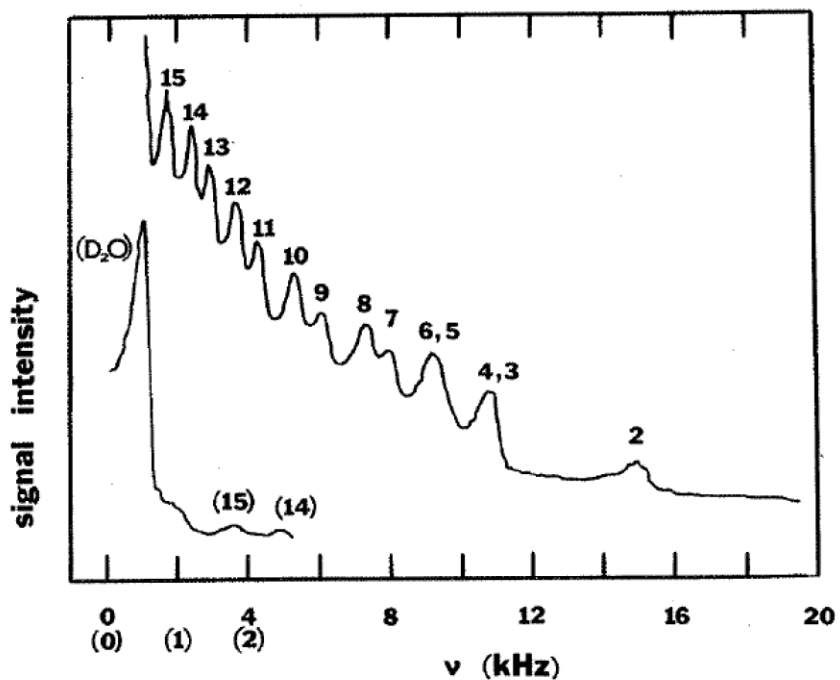

FIG. 2. The deuterium nmr half-spectrum of the 5% C_{22} sample at 145°C. The peaks are labelled by carbon position along the chain. The D_2O, 15, and 14 position peaks shown in parentheses at the lower left correspond to the expanded scale shown in parentheses on the abscissa.
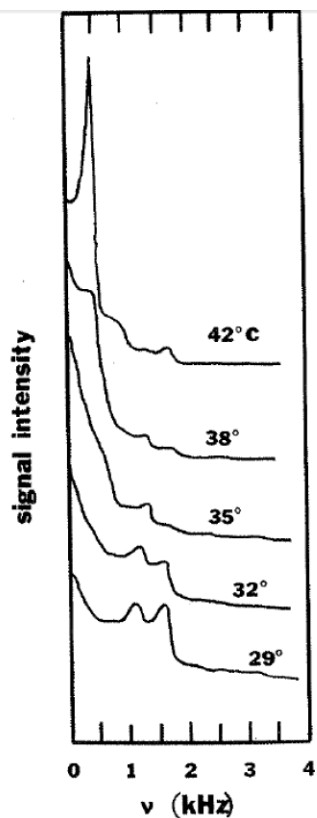
FIG. 3. The central part (low frequency) of the deuterium nmr half-spectra showing the D_2O signals from the 20% C_{22} sample at various temperatures below T_c.
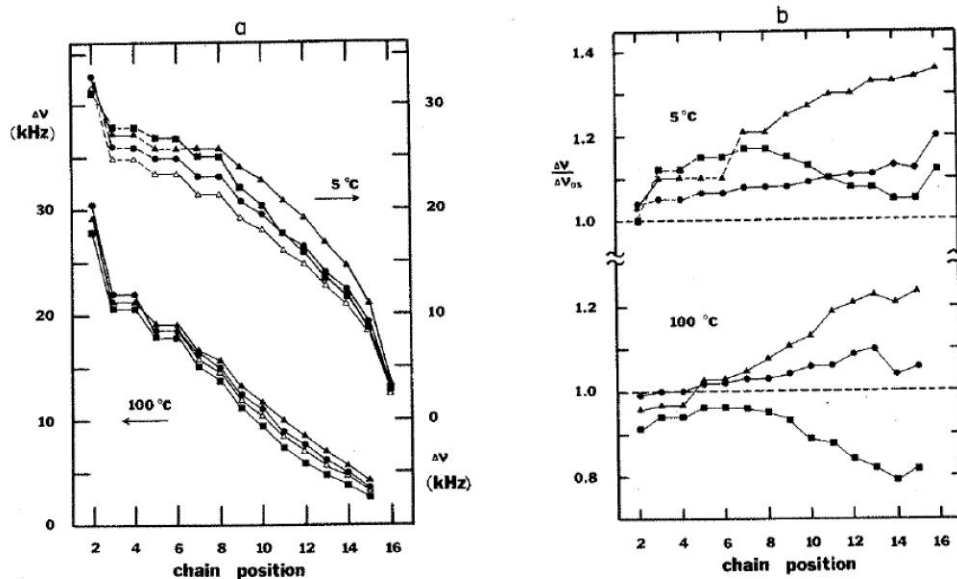
FIG. 4. Perdeuterated potassium palmitate deuterium nmr splittings and splitting ratios as a function of carbon position at the reduced temperatures of 5 and 100°C. The splittings are shown in a where the right-hand ordinate scale corresponds to $T_r = 5$°C and the left-hand ordinate scale corresponds to $T_r = 100$°C. The ratios of the splittings to those of the 0% sample are shown in b. The symbols refer to the 0% sample ($\triangle$), the 5% C_{22} sample ($\bullet$), the 20% C_{22} sample ($\blacktriangle$), and the 20% C_8 sample ($\blacksquare$). The solid lines are for visual clarity only. Dotted lines surround points of doubtful assignment (for $T_r = 5$°C). For carbon positions 1 to 6 the 0% sample data points at 100°C in a are plotted in the same position as the 5% C_{22} data points. This has been done for clarity and the small difference in these values can be seen by investigating b.
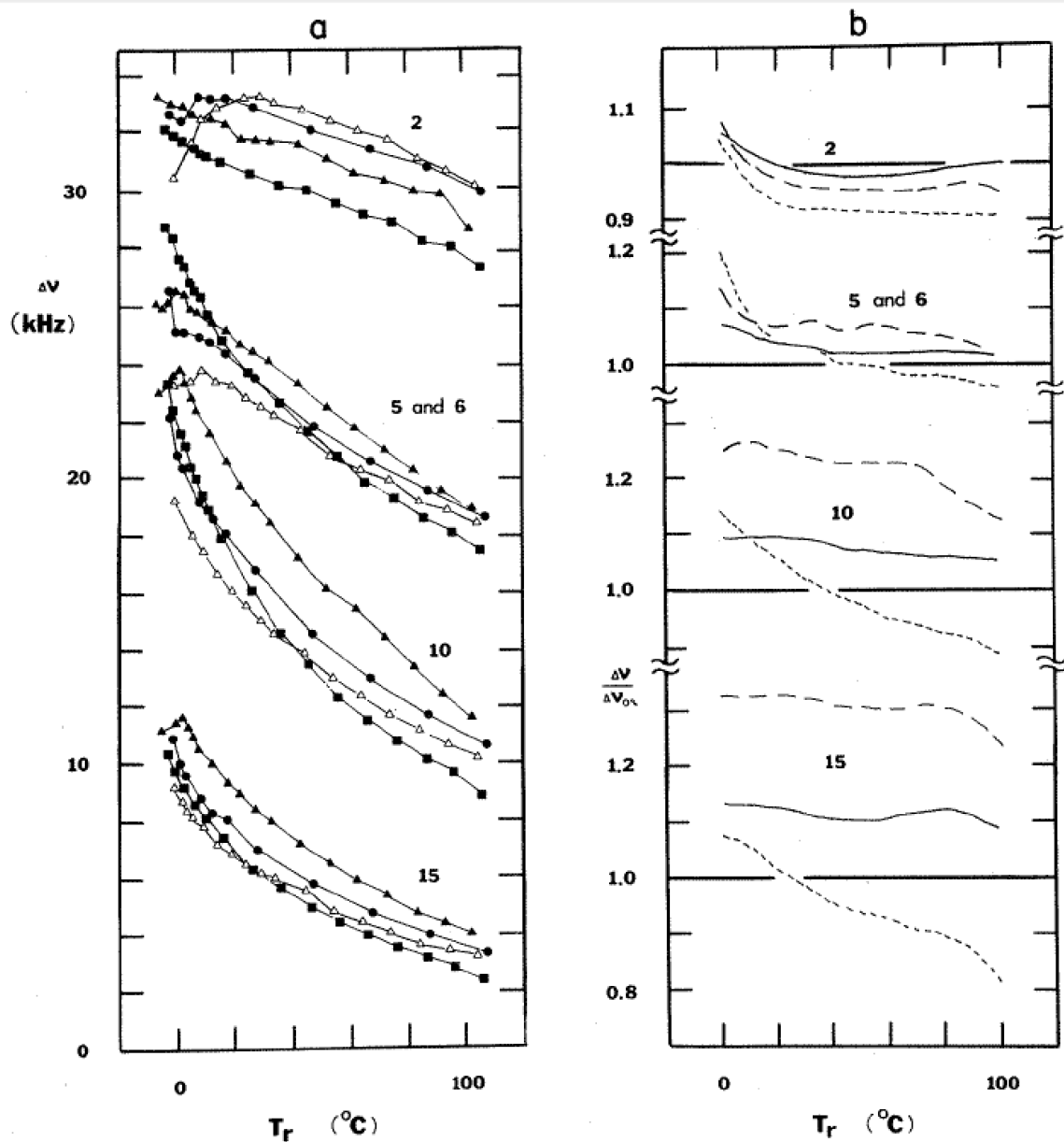
FIG. 5. Perdeuterated potassium palmitate deuterium nmr splittings Δν and ratios Δν/Δν$_{0\%}$ as a function of reduced temperature T_r for various carbon positions as indicated. The absolute splittings Δν are shown in *a* for the 0% sample (△), the 5% C$_{22}$ sample (●), the 20% C$_{22}$ sample (▲), and the 20% C$_8$ sample (■). The ratios of the splittings to the splittings in the 0% sample Δν/Δν$_{0\%}$ are shown in *b* for the 5% C$_{22}$ sample (——), the 20% C$_{22}$ sample (———), and the 20% C$_8$ sample (- - -).
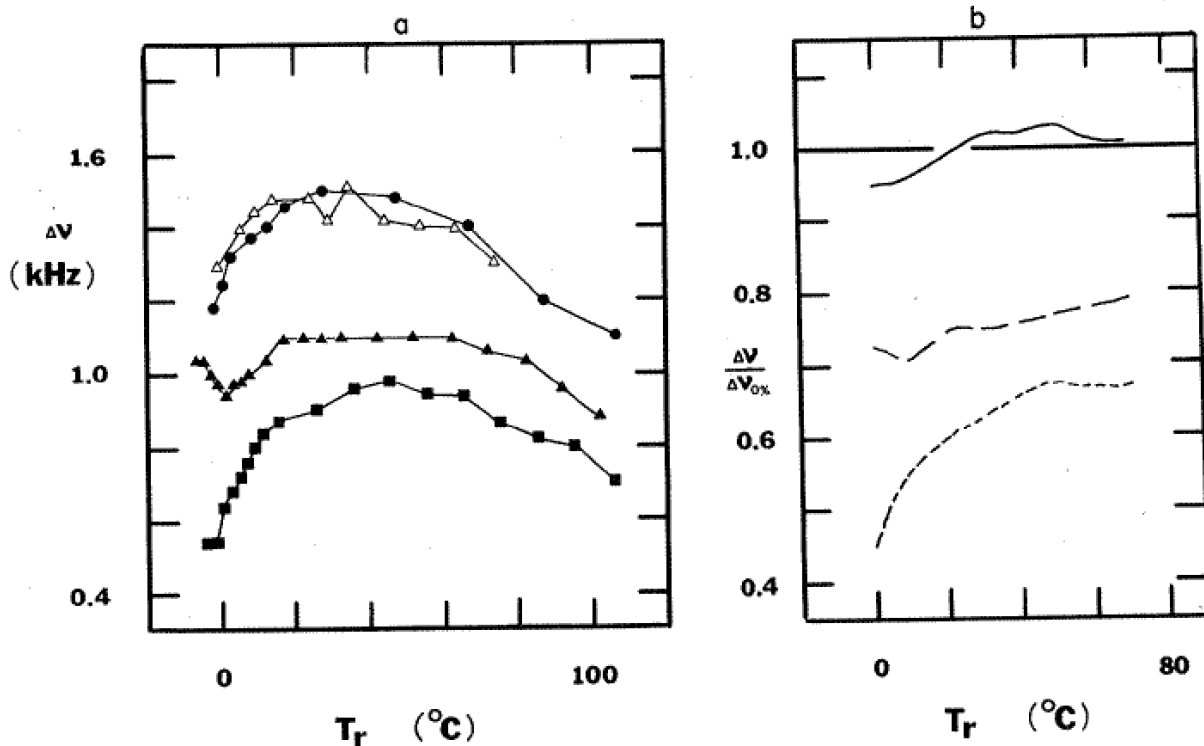
FIG. 6. D_2O deuterium nmr splittings Δv and ratios $\Delta v/\Delta v_{0\%}$ as a function of reduced temperature T_r. The absolute splittings Δv are shown in a for the 0% sample ($\triangle$), the 5% C_{22} sample ($\bullet$), the 20% C_{22} sample ($\blacktriangle$), and the 20% C_8 sample ($\blacksquare$). The ratios of the splittings to the splittings in the 0% sample $\Delta v/\Delta v_{0\%}$ are shown in b for the 5% C_{22} sample (——), the 20% C_{22} sample (——), and the 20% C_8 sample (---).
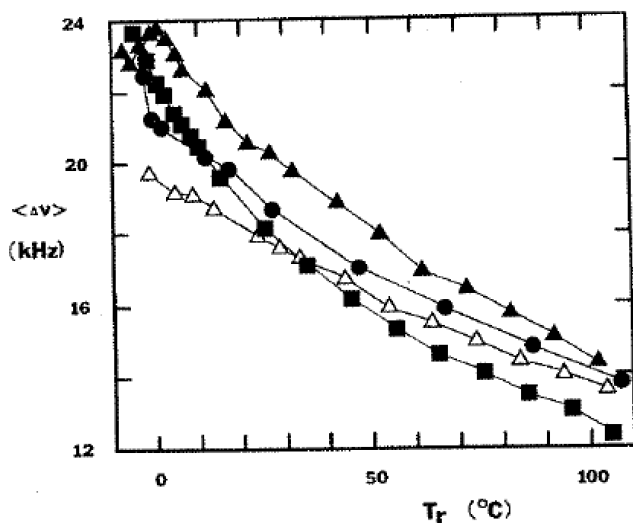

FIG. 7. The average value $\langle \Delta v \rangle$ of the perdeuterated potassium palmitate splittings Δv_i given by [1] in the text as a function of reduced temperature T_r for the 0% sample ($\triangle$), the 5% C_{22} sample ($\bullet$), the 20% C_{22} sample ($\blacktriangle$), the 20% C_8 sample ($\blacksquare$).
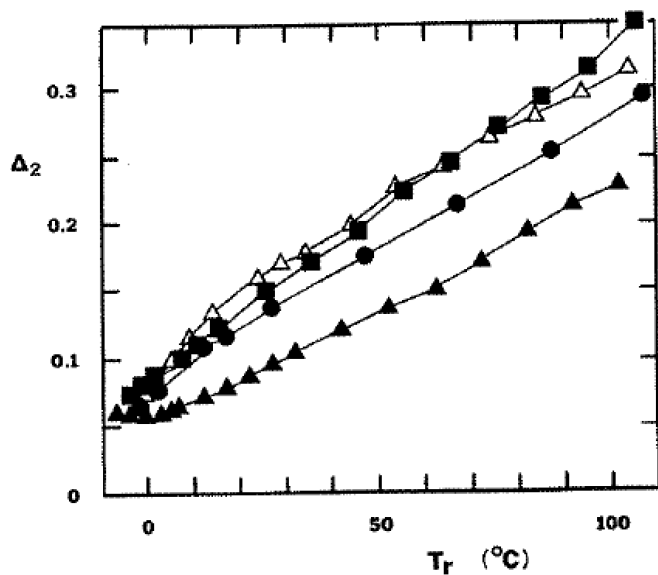
FIG. 8. The distribution parameter Δ_2 of the perdeuterated potassium palmitate given by [3] in the text as a function of reduced temperature T_r for the 0% sample ($\triangle$), the 5% C_{22} sample ($\bullet$), the 20% C_{22} sample ($\blacktriangle$), and the 20% C_8 sample ($\blacksquare$).
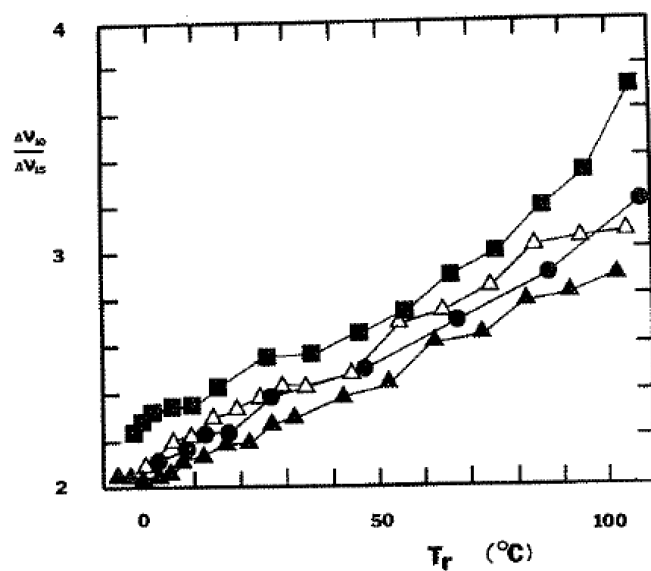

FIG. 9. The ratio of the perdeuterated potassium palmitate splittings for carbon position 10 to that of carbon position 15 as a function of reduced temperature T_r for the 0% sample ($\triangle$), the 5% C_{22} sample ($\bullet$), the 20% C_{22} sample ($\blacktriangle$), and the 20% C_8 sample ($\blacksquare$).
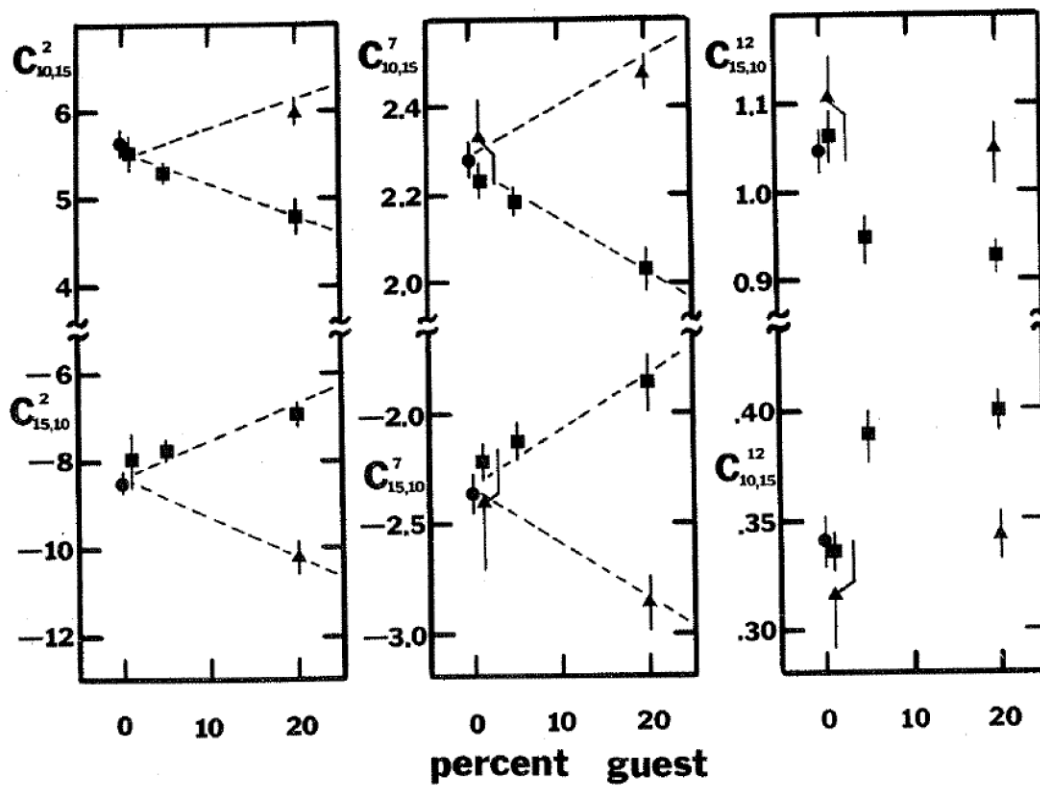
FIG. 10. Value of $C_{10,15}{}^i$ and $C_{15,10}{}^i$ for $i = 2, 7,$ and 12 as a function of percent guest molecule. The symbols refer to 0% (●), % C_{22} (■), and % C_8 (▲). The pairs of dashed lines in C^2 and C^7 have equal and opposite slopes.

Tables

TABLE 1. Composition and phase transition temperature of samples

Sample	Mol% D_2O	Mol% K-octanoate	Mol% perdeuterated K-palmitate	Mol% K-behenate	T_c (°C)
0%	86.3	—	13.7	—	41
1% C_8	86.3	0.14	13.6	—	41
20% C_8	86.3	2.7	11.0	—	40
1% C_{22}	86.3	—	13.6	0.14	41
5% C_{22}	86.3	—	13.0	0.68	38
20% C_{22}	86.3	—	11.0	2.7	43